J Mater Sci: Mater Med (2008) 19:1669–1679
DOI 10.1007/s10856-007-3313-1

Processing, characterisation, and biocompatibility of zinc modified metaphosphate based glasses for biomedical applications

Ensanya Ali Abou Neel · Luke Austin O'Dell · Mark Edmund Smith · Jonathan Campbell Knowles

Received: 21 September 2007 / Accepted: 10 October 2007 / Published online: 1 December 2007

Abstract Bulk and structural properties of zinc oxide (0 up to 20 mol%) containing phosphate glasses, developed for biomedical applications, were investigated throughout this study using differential thermal analysis (DTA), differential scanning calorimetry, X-ray powder diffraction and ^{31}P and ^{23}Na MAS NMR. Surface wettability and MG63 viability were also considered for surface characterisation of these glasses. The results indicated that incorporation of zinc oxide as a dopant into phosphate glasses produced a significant increase in density; however, the thermal properties presented in glass transition, and melting temperatures were reduced. $NaZn(PO_3)_3$ was detected in the X-Ray Powder Diffraction Analysis (XRD) trace of zinc containing glasses, and the proportion of this phase increased with increasing zinc oxide content. $NaCa(PO_3)_3$ as a second main phase and CaP_2O_6 in minor amounts were also detected. The ^{31}P and ^{23}Na MAS NMR results suggested that the relative abundances of the Q^1 and Q^2 phosphorus sites, and the local sodium environment were unaffected as CaO was replaced by ZnO in this system. The replacement of CaO with ZnO did seem to have the effect of increasing the local disorder of the Q^2 metaphosphate chains, but less so for the Q^1 chain-terminating sites which were already relatively disordered due to the proximity of modifying cations. Glasses with zinc oxide less than 5 mol% showed higher surface wettability, while those with 5 up to 20 mol% showed comparable wettability as zinc oxide free glasses. Regardless of the high hydrophilicity and surface reactivity of these zinc oxide containing glasses, they had lower biocompatibility, in particular 10–20 mol% ZnO, compared to both zinc free glasses and Thermanox®. This may be associated with the release of significant amount of Zn^{2+} enough to be toxic to MG63.

E. A. Abou Neel · J. C. Knowles (✉)
Division of Biomaterials and Tissue Engineering, UCL Eastman Dental Institute, 256 Gray's Inn Road, London WC1X 8LD, UK
e-mail: j.knowles@eastman.ucl.ac.uk

L. A. O'Dell · M. E. Smith
Department of Physics, University of Warwick, Coventry CV4 7AL, UK

1 Introduction

Currently, bioactive and biodegradable materials which are able to stimulate specific and controlled cell responses at the molecular level are of major interest as scaffolds for tissue engineering applications [1]. Phosphate based glasses have the potential to be used as scaffold materials since they are degradable due to the abundance of the easily hydrated-P–O–P bonds, and their degradation products are natural constituents which can be tolerated by the body [2]. Additionally, their degradation is strongly compositional dependant, and accordingly a wide range of compositions with various degradation rates can be tailored [3, 4] according to the end use.

All attempts made to harmonise the degradation behaviour with an end application depend on using different modifying oxides such as Fe_2O_3 [5–8], CuO [9], Al_2O_3 [10], TiO_2 [11–14] and ZnO [15]. These oxides have been incorporated into the ternary P_2O_5–CaO–Na_2O glass at the expense of Na_2O or CaO, and yielded glass systems with relatively low degradation compared to the parent ternary compositions. Incorporation of these oxides was also to induce a specific function. For example, controlling Ca/P ratio has been attempted to produce compositions

close to hydroxyapatite for proper osseointegration into the surrounding tissues [16].

Zinc oxide was found to be effective in controlling the chemical durability and bioactivity of glass-ceramics in terms of apatite layer formation which is generally considered essential for attachment of osteoblast cells as a starting step towards bone formation [17]. Moreover, as an element, zinc was found to be important for bone formation. It is well known that zinc deficiency in humans is associated with dysfunction of the cellular immune system which can result of severe microbial infections [18]. Therefore, zinc oxide was also incorporated into the native titanium oxide layer formed on the surface of titanium implants to impart beneficial properties into the surface of the implant with the possibility of preventing bacterial colonisation responsible for implant failure [19].

In this study, we have developed phosphate glasses of calcium phosphate incorporating sodium, calcium, and zinc oxide proposed as substitute for bone tissue regeneration. In a previous study [15], incorporation of ZnO into phosphate glasses was attempted at the expense of CaO. Cyquant assay, carried out only on glasses with ZnO up to 5 mol%, was used to assess the effect of the dissolution products of these glasses (neat and 10% diluted extracts) on proliferation of MG63 cells for up to 7 days. The results showed that the proliferation rate increased with time for these glasses; however, it is also essential to determine the behaviour of cells in direct contact with the material surface. Therefore, viability of MG63 cells seeded on the surface of glass compositions with ZnO up to 20 mol% was attempted in this study. In addition, the effect of substitution of CaO with ZnO was considered on the bulk, structural, and surface properties.

2 Experimental

2.1 Glass preparation

The precursors used in the preparation of these glasses were sodium dihydrogen orthophosphate (NaH_2PO_4), calcium carbonate ($CaCO_3$), phosphorus pentoxide (P_2O_5), and zinc oxide (ZnO) (BDH, Poole, UK). These were placed in a Pt/10%Rh crucible (Type 71040, Johnson Matthey, Royston, UK) which was introduced into a pre-heated furnace (Carbolite, RHF 1500, Sheffield, UK) at 550 °C to allow for removal of H_2O and CO_2 then followed by melting at 1,100 °C for 1 h. The compositions used in this study are given in Table 1. Upon removal of the crucible from the furnace, the melted glass was then poured into a pre-heated graphite mould at 350 °C for 1 h. The mould was then allowed to cool to room temperature in the furnace overnight. Rods of 15 mm diameter for each composition were then sectioned into approximately 2 mm thick discs using a Testbourne diamond saw and methanol as a coolant/lubricant.

Table 1 Glass codes and compositions used throughout this study

Glass code	Glass composition (mol%)			
	Phosphorous pentoxide	Calcium oxide	Sodium oxide	Zinc oxide
P50 Ca40Na10	50	40	10	0
P50Ca39Na10Zn1	50	39	10	1
P50Ca38Na10Zn2	50	38	10	2
P50Ca37Na10Zn3	50	37	10	3
P50Ca36Na10Zn4	50	36	10	4
P50Ca35Na10Zn5	50	35	10	5
P50Ca30Na10Zn10	50	30	10	10
P50Ca25Na10Zn15	50	25	10	15
P50Ca20Na10Zn20	50	20	10	20

2.2 Bulk glass characterisation

2.2.1 Density measurements

Density measurements were conducted on triplicate samples using Archimedes' Principle, on an analytical balance (Mettler Toledo, UK) with an attached density kit. Due to the soluble nature of the glass compositions investigated, ethanol was used as the submersion liquid for these measurements. The density of the glasses (ρ) were obtained employing the following equation,

$$\rho = \left(\frac{M_{dry}}{M_{dry} - M_{wet}}\right) \times \rho_{liquid}$$

where: M_{dry} and M_{wet} are the masses of sample in air and liquid respectively, and ρ_{liquid} is density of ethanol at room temperature.

2.2.2 Thermal analysis

(I) Differential Scanning Calorimetry A portion of each glass sample was crushed into powder, and the glass transition temperature (T_g) was determined using a Pyris Diamond DSC (Perkin–Elmer Instruments, UK). The instrument was calibrated using the manufacturer's instructions, with indium and zinc as standards, and all tests were carried out under nitrogen purge. Samples ($n = 3$) of 5 mg were heated, cooled and reheated from 25 °C to 550 °C at 100 °C min^{-1}. T_g was calculated by the onset of change in the endothermic direction (upwards) of the heat flow.

(II) Differential Thermal Analysis Differential Thermal Analysis (DTA) was carried out using a Setaram Differential Thermal Analyser (Setaram, France) on powdered glass samples of approximately 60 mg. Three main thermal parameters were measured; T_g, crystallisation temperature (T_c), and melting temperature (T_m). An increase in temperature from ambient up to 1,000 °C at a heating rate of 6.7 °C min^{-1} was carried out under nitrogen purge; an empty platinum crucible was used as a reference. The data were baseline corrected by carrying out a blank run, and subtracting this from the original data.

2.2.3 X-ray powder diffraction

For X-Ray Powder Diffraction Analysis (XRD), the glass compositions were crystallised at those temperatures obtained through the DTA. The data were collected on a Brüker D8 Advance Diffractometer (Brüker, UK) in flat plate geometry, using Ni filtered Cu Kα radiation and a Brüker Lynx Eye detector. Data were collected from 10° to 100° 2θ with a step size of 0.019962° and a count time of 0.1 s. The phases were identified using the Crystallographica Search-Match (CSM) software (Oxford Cryosystems, Oxford, UK) and the International Centre for Diffraction Data (ICDD) database (vols. 1–42).

2.2.4 ^{23}Na and ^{31}P MAS NMR study

^{23}Na MAS NMR experiments were conducted using a 3.2 mm diameter rotor spinning at 30 kHz. Spectra were acquired using a Bruker Avance II spectrometer attached to a 14.1 T magnet (^{23}Na Larmor frequency 158.7 MHz). Aqueous NaCl was used as a reference, with the sharp resonance from this set to 0 ppm. The liquid 90° pulse length was determined to be 2.5 μs, although a much shorter pulse length (0.5 μs) was used on the solid samples. A one-pulse sequence was used, with a recycle delay of 5 s. Certain ^{23}Na spectra were also obtained at 7.05 or 8.45 T using a 4 mm diameter rotor spinning at 12.5 kHz, with similar pulse lengths and recycle delays.

^{31}P MAS NMR experiments were conducted using a 4 mm diameter rotor spinning at 10–12.5 kHz. Spectra were acquired using a Chemagnetics Infinity Plus spectrometer attached to a 7.05 T magnet (^{31}P Larmor frequency 121.5 MHz). $NH_4H_2PO_4$ was used as a secondary reference compound, the signal from this set to 0.9 ppm. A pulse length of 1.5 μs was used (corresponding to a ~30° tip angle), with a recycle delay of 5 s.

All NMR spectra were processed using either TOPSPIN 2.0 or Spinsight and fitted using either dmfit2007 [20] or QuadFit [21].

2.3 Substrate surface characterisation

2.3.1 Wettability and surface free energy

Glass discs from each composition were abraded and polished using waterproof silicon carbide papers (P # 1200, Struers). Static contact angle for the test liquids, ultra-pure water and diiodomethane that were used to represent both polar and non-polar characteristics respectively, was measured using a KSV Cam200 contact angle system (L. O. T-Oriel, Ltd., UK). Droplets of approximately 5 μL of the test liquids were placed on the glass surface using a manual syringe. The drop profile was recorded at 0.1 s intervals for 1 min, and the measurements were carried out on triplicate samples. Prior to each measurement, the samples were ultra-sonicated in ethanol for 5 min and allowed to dry. The calculation of the surface free energy was carried out using OWRK method via KSV software.

2.3.2 Biological assessment

In vitro viability study using human osteosarcoma cell line (MG63) was conducted up to 5 days to assess the biocompatibility of ZnO containing glasses and compared with both ZnO free glass and Thermanox® positive controls. All samples for biocompatibility studies were sterilised by heating at 180 °C for 3 h, and pre-treated by incubation in a growth medium described below for 24 h at 37 °C humified atmosphere incubator of 5% CO_2 in air.

(I) Cell Culture: MG63 cells were cultured at 37 °C humified atmosphere incubator of 5% CO_2 in air, in a growth medium [Dulbecco's modified Eagles Medium (DMEM, Gibco), 10% fetal calf serum, and 1% penicillin and streptomycin solution (Gibco)]. The medium was changed every 3 days. The cells were seeded on the surface of the glass discs of various compositions and Thermanox® at a density of 3×10^4 cells/disc in a 6-well culture plates.

(II) Cell Viability and Live Dead Staining: Determination of cell viability was carried out by incubating the discs and the controls for 1 h in a standard growth medium containing 1 μL/mL calcein AM, to stain the live cells, and propidium iodide, to stain the dead cells. Live cells cleave membrane-permeant calcein AM to yield cytoplasmic green fluorescence; membrane-impermeant propidium iodide labels nucleic acids of membrane compromised cells with red fluorescence. The assessment of cell viability in three dimensions was performed using confocal microscopy (Bio-Rad, USA). In a typical scan, the sample was placed into the bottom of a 35 mm culture dish, and sections of the sample were scanned using a 20× lens. The region of interest was 600 × 600 μm, *x*–*y* dimension, and the images were collected at 2 μm intervals through the

thickness of the cell sheet formed on the top of the surface in z-dimension (z-stacks) using Laser Sharp 2000 software. Excitation wavelengths for the fluorescent dyes for live and dead cells were provided at 488 nm from an argon laser and 543 nm from a Green/HeNe laser respectively. Projection images were created by superimposing the z-stack images that were captured throughout the construct thickness using ImageJ software (National Institute of Health).

3 Results and discussion

3.1 Bulk characterisation

3.1.1 Density

Figure 1 shows the density (g cm^{-3}) as a function of ZnO contents; it was observed that the density of the bulk glass increased linearly with increasing ZnO contents. It increased from 2.63 ± 0.01 to 2.78 ± 0.01 g cm^{-3} by incorporation of 20 mol% ZnO into the ternary P50C40N10 glass formulation (0 mol% ZnO). This finding suggested that addition of ZnO at the expense of CaO increases the atomic packing in the produced glasses structure. This may be associated with the fact that Zn^{2+} ions have smaller radius (88 pm) than Ca^{2+} ions (114 pm), therefore, they reduce the inter-atomic spacing particularly the atomic volume of Zn^{2+} (9.2 cm^3 mol^{-1}) is approximately three times lower than that of Ca^{2+} (29.9 cm^3 mol^{-1}). Moreover, the density of Zn^{2+} (7.14 g cm^{-3} @ 293 K) is approximately five times higher than that of Ca^{2+} (1.55 g cm^{-3} @ 293 K) [22].

3.1.2 Thermal analysis

Unlike density, the glass transition temperature, which is a measure of the bulk properties, reduced linearly with increasing ZnO content into the glass structure; this trend was observed from both DSC and DTA as seen in Fig. 2. From the DTA data, T_g was also reduced from 437.9 for 0 mol% ZnO glasses to 370.7 °C for 20 mol% ZnO glasses; these findings were correlated well with those obtained previously [15, 17]. From DSC, however, the T_g was reduced from 455.0 ± 0.7 for 0 mol% ZnO glasses to 384.8 ± 0.6 °C for 20 mol% ZnO glasses. The significant differences between DSC and DTA results could be associated with the difference in the heating rate used for both techniques. As expected, higher heating rates resulted in higher transition temperatures. Since T_g was used as a measure of bond strength and the cross-link density of the glass structure [23], the reduction in T_g observed with increasing ZnO content gave an indication that Zn–O–P bonds are weaker than Ca–O–P bonds, and also the cross-link density of glasses with high ZnO content was lower than that of ZnO free glasses.

Unlike DSC, DTA analysis shown in Fig. 3 provides more information at temperatures higher than 600 °C; the DTA for 0 mol% ZnO glasses showed the presence of a single sharp crystallisation and melting peak. Incorporation of ZnO up to 4 mol% resulted in broadening of the crystallisation peak, however, this peak started to be well defined again with further addition of ZnO. The crystallisation temperature increased by approximately 20 °C with addition of 1 mol% ZnO, and it was increased by 50 °C with addition of 2, 3, and 4 mol% ZnO into the ternary composition. While the addition of ZnO beyond 4 mol% did not produce any significant changes in the crystallisation temperature compared to the ternary composition. Like T_g, the melting temperature was linearly reduced with addition of ZnO into the ternary glasses. These observations were also correlated well with those obtained from other work [15] regardless of the difference in the heating rate. The DTA data were useful in identifying the crystallisation temperatures used for preparing samples for

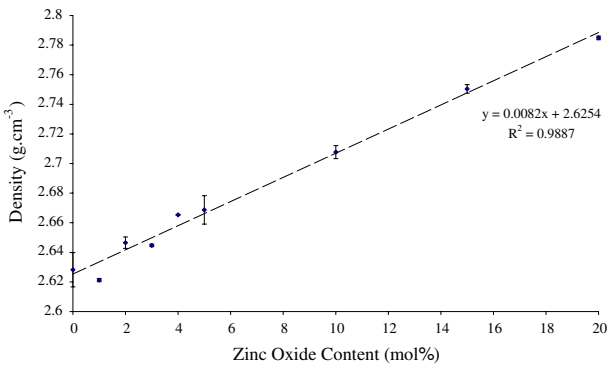

Fig. 1 Density (g cm^{-3}) of phosphate glasses as a function of zinc oxide content (mol%)

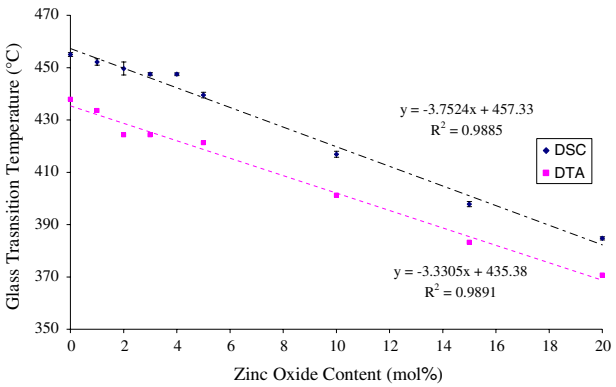

Fig. 2 Glass transition temperature (°C) of phosphate glasses as a function of zinc oxide content (mol%) as measured by DSC and DTA

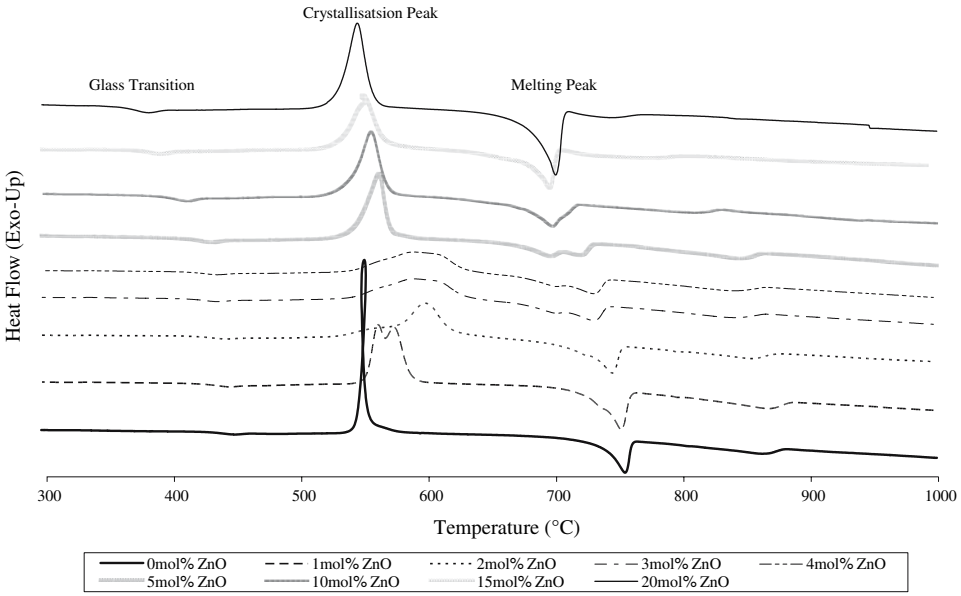

Fig. 3 DTA trace of phosphate glasses doped with different zinc oxide contents

identification of the crystalline phases in the parent structure through XRD.

3.1.3 X-ray powder diffraction

XRD was carried out only for glasses with 0, and 5–20 mol% ZnO, as an example, to study the crystalline phases of them. For the ternary glass with no ZnO (P50Ca40Na10), a $NaCa(PO_3)_3$ (ICCD no. 23-669) was identified as the main phase from the Crystallographica database, and CaP_2O_6 (ICCD no. 1139) as the second main phase. With incorporation of ZnO into this composition, $NaZn(PO_3)_3$ (ICCD no. 24-1168) became the main phase, and the $NaCa(PO_3)_3$ phase the second main phase, while CaP_2O_6 was detected in minor amounts. Generally, the proportion of $NaZn(PO_3)_3$ increased with increasing ZnO content.

3.1.4 ^{23}Na and ^{31}P MAS NMR study

Figure 4 shows a stacked plot of the ^{31}P MAS NMR spectra obtained from the glass samples, with the horizontal frequency scale expanded about the isotropic region such that the spinning sidebands are not shown. In all the spectra, two peaks are visible, a low intensity peak centred at approximately −10 ppm and a much larger peak centred at around −26 ppm. These peaks represent phosphorus atoms in Q^1 and Q^2 sites respectively. In order to obtain the relative abundances of each of these Q^n species, the intensities of these peaks were fitted (along with the spinning sidebands). An example of such fitting is shown in

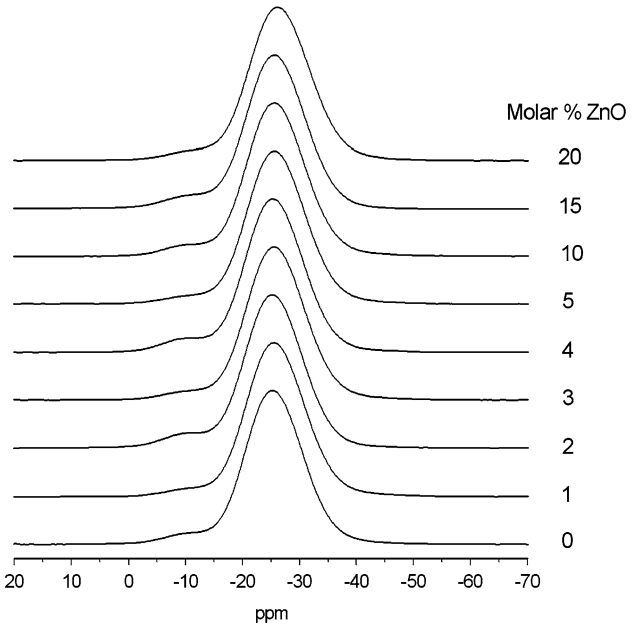

Fig. 4 The ^{31}P MAS NMR spectra obtained from the glass samples, with the horizontal frequency scale expanded to show just the isotropic region

Fig. 5 and the relative abundances of the Q^2 species is shown in Fig. 6. As can be seen, there is no linear trend in the relative abundances of the Q^n species as the molar % of ZnO in the glasses is increased from 0 to 20, and the amount of Q^2 present remains at roughly 94%. No Q^3 or Q^0 sites were observed in any of the spectra.

Figure 7 shows how the ^{31}P MAS NMR chemical shifts and linewidths of the Q^1 and Q^2 sites varied with the increasing ZnO content. Figure 7a and c shows that the

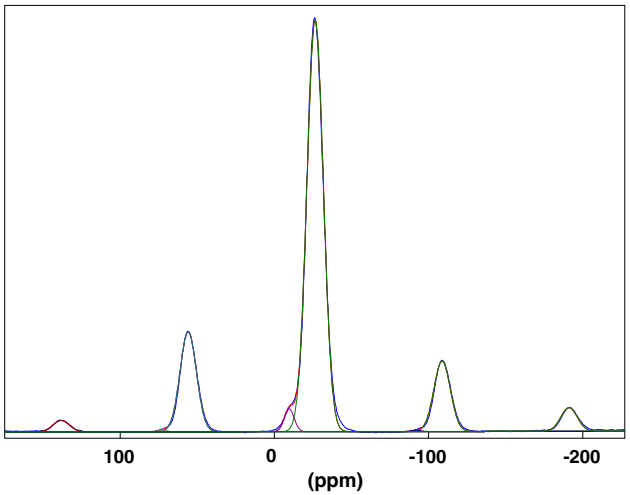

Fig. 5 Fit of the ^{31}P MAS NMR spectrum obtained from the 20 mol% ZnO metaphosphate glass

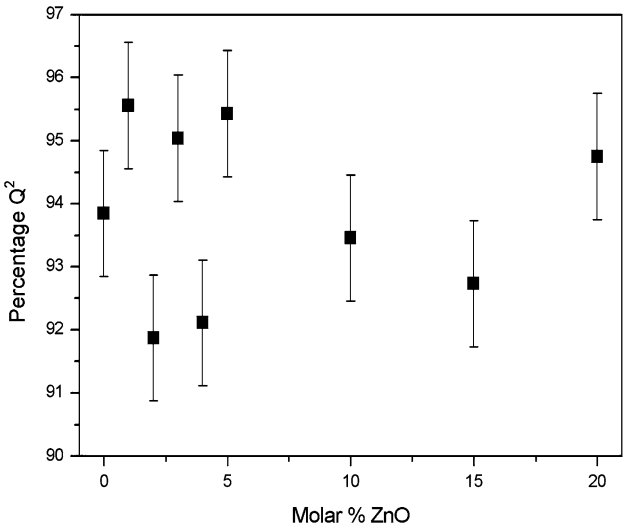

Fig. 6 The abundance of the Q^2 site in the metaphosphate glasses with increasing molar % ZnO

chemical shifts for both sites moved to a more negative shift at higher ZnO concentrations. No linear trend was observed for the Q^1 linewidth (Fig. 7b), whereas the Q^2 linewidth clearly showed an increase for the 20 mol% ZnO sample (Fig. 7d).

Figure 8a shows the ^{23}Na MAS NMR spectra obtained from the samples. The spectra all show a single broad peak, which remains constant as the ZnO content increases. This peak can be fitted (despite the lack of sharp features) by using multiple-field data and simulating a Gaussian distribution in the quadrupolar coupling constant C_Q (FWHM of this distribution = ΔC_Q), which can be used as a quantitative measure of disorder [24]. An example of such fitting is shown in Fig. 8b. The spectra were simulated with a mean $C_Q = (2.55 \pm 0.1)$ MHz, $\Delta C_Q = (2.10 \pm 0.1)$ MHz, and an isotropic chemical shift of (-7 ± 1) ppm. These parameters gave a good fit to all of the ^{23}Na MAS NMR lines in Fig. 8a. For simplicity, the isotropic chemical shift was kept constant, and the asymmetry parameter η_Q was set at 0, though in reality a distribution in C_Q would likely mean a distribution in these parameters also.

The dominance of the Q^2 peak in the ^{31}P MAS NMR spectra in Fig. 4 is to be expected since phosphate glasses containing 50 mol% P_2O_5 are well known to consist almost entirely of infinite chains or loops of phosphate tetrahedra [25]. Increasing the ZnO content had little effect on the relative abundances of the Q^1 and Q^2 peaks to within experimental uncertainty. This is because in these samples the ZnO replaces the CaO in the system, so the amount of P_2O_5 remains constant and no depolymerisation takes place. Increasing the ZnO content did have a visible effect on the ^{31}P MAS NMR chemical shifts however, with both the Q^1 and Q^2 peaks moving to a more negative chemical shift as the calcium was replaced by the zinc. This is consistent with the observation reported by Brow et al. [26] that as the cation potential (charge to radius ratio) of the modifying cation increases, the phosphorus chemical shift becomes more negative (zinc has a larger cation potential than calcium). The same reference also reports that the linewidths should increase with increasing cation potential, and this is indeed observed for the Q^2 peak in Fig. 7d. This increase in Q^2 linewidth is indicative of increasing disorder in the system (i.e., larger distributions in P–O–P bond lengths and angles in the phosphate chains). The fact that the Q^1 linewidths did not seem to generally increase with increasing ZnO content may be due to the fact that these Q^1 phosphorus environments were already relatively disordered compared to the Q^2 sites due to their close proximity to the Na^+ modifying cations. The ^{23}Na MAS NMR results in Fig. 8a show that the distributions in sodium environments remained constant over the range of compositions studied.

3.2 Surface characterisation

3.2.1 Wettability and surface free energy

This study investigated the surface wettability by using static contact angle measurements which normally used to characterise the top 0.5 nm of the material surface. This surface layer is important in determining the level of interaction between the biomaterial and cells. Generally, glasses were considered to have high surface energy i.e., can be easily wetted with water, and tend to absorb low energy compounds available in the surrounding environments such as proteins which may be essential for cell adhesion [27, 28].

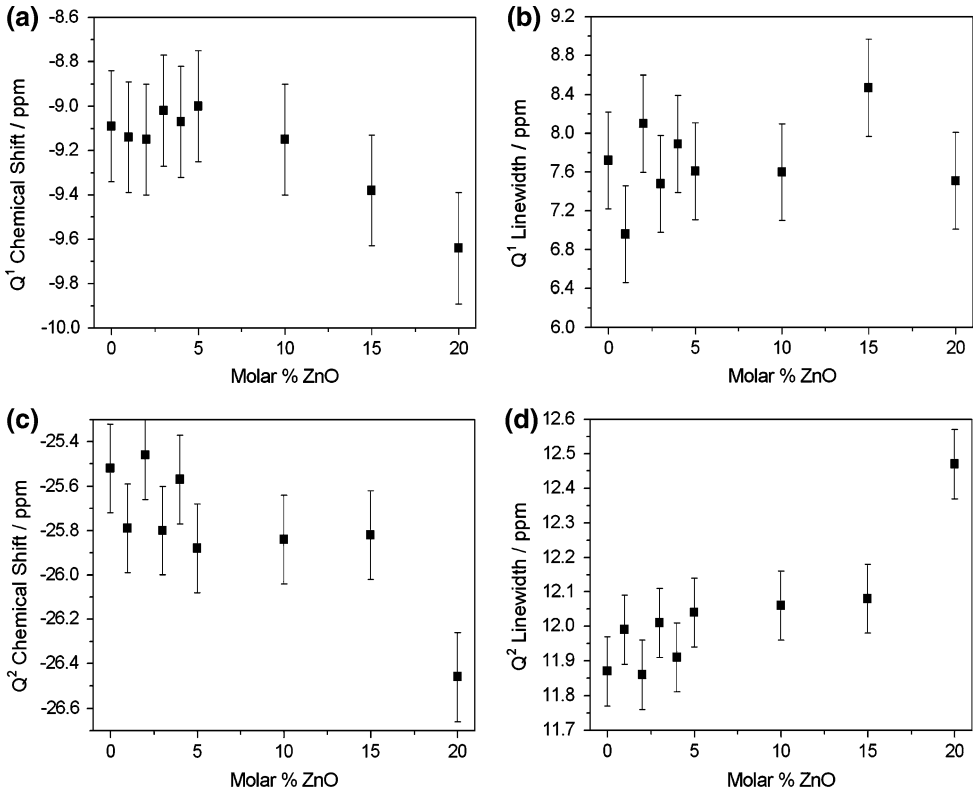

Fig. 7 The variation in ^{31}P MAS NMR chemical shift and linewidth for the Q^1 (**a** and **b**) and Q^2 (**c** and **d**) species in the metaphosphate glasses. The experimental uncertainties are larger for the Q^1 peaks due to their relatively low intensity

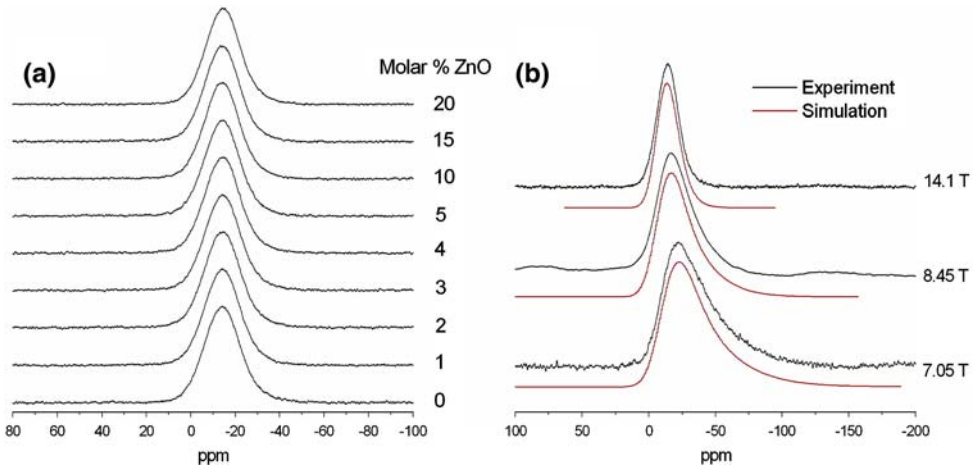

Fig. 8 (**a**) The ^{23}Na MAS NMR spectra obtained from the metaphosphate glasses at 14.1 T, and (**b**) simulated spectra of the 0% ZnO sample at 14.1, 8.45 and 7.05 T

The contact angle of a liquid is determined by the interactions of this liquid with a solid surface. It is usually expected that a liquid with a lower surface tension will give rise to a smaller contact angle on a given solid when compared to a liquid with a higher surface tension. Ultra-pure water and diiodomethane were used as two liquids representing polar and non-polar characteristic respectively, and this study investigated the interaction of the studied glasses with these two test liquids. The mean contact angle and standard deviations are listed in Table 2. It can be seen from the results that the contact angle of water and Thermanox® is higher than that with diiodomethane. However, this was not the case with the glasses, since the lowest contact angles were obtained for water on all studied glass surfaces even though water has a higher surface tension than diiodomethane, indicating the dominating effect was the polar characteristic of phosphate glasses. This polarity can be attributed to the P–O–P bonds in the glass, and this was also supported in our previous study [4].

With water as a polar test liquid, all the studied glass compositions showed significantly lower contact angles than Thermanox® i.e., relatively hydrophilic. Addition of

Table 2 Total surface free energy (SFE^{tot} in mN m^{-1}) with the dispersive (SFE^{d}) and polar part (SFE^{p}) of phosphate glasses with different zinc oxide contents and Thermanox® according to OWRK method, and contact angle measurements (°) for ultra-pure water (CA^{H_2O}) and diiodomethane (CA^{DII}) as test liquids

Sample	SFE^{d}	St Dev	SFE^{p}	St Dev	SFE^{tot}	St Dev	CA^{H_2O} (°)	St Dev	CA^{DII} (°)	St Dev
Thermanox®	33.8	0.66	5.35	0.26	39.15	0.93	78.43	1.18	56.63	5.99
P50 Ca40Na10	34.7	5.4	32.55	5.57	67.25	4.32	33.93	1.21	48.99	9.87
P50Ca39Na10Zn1	33.58	2.0	35.94	0.91	69.52	1.49	23.11	2.31	51.37	3.41
P50Ca38Na10Zn2	32.46	4.17	39.67	2.81	72.13	1.36	15.19	0.95	53.14	7.38
P50Ca37Na10Zn3	33.34	3.87	35.4	1.81	68.74	2.41	24.77	3.0	51.58	6.84
P50Ca36Na10Zn4	33.21	2.1	36.01	1.61	69.22	2.15	26.31	2.56	54.54	3.48
P50Ca35Na10Zn5	30.98	1.83	35.5	2.39	66.49	4.21	27.59	6.39	54.47	3.23
P50Ca30Na10Zn10	36.93	1.83	26.65	2.36	63.58	0.53	37.62	2.4	47.11	4.22
P50Ca25Na10Zn15	34.26	4.69	36.75	4.88	71.01	1.21	19.94	5.43	49.86	8.49
P50Ca20Na10Zn20	32.67	4.74	26.51	0.99	59.17	5.52	41.61	5.88	52.76	8.47

ZnO up to 5 mol% produced a significant reduction ($p < 0.05$) in the mean contact angles compared to 0 mol% ZnO glass. This finding suggested that glasses with ZnO up to 5 mol% have relatively higher surface wettability compared to 0 mol% ZnO glass. Further addition of ZnO up to 20 mol%; however, produced no significant differences in the contact angle compared to 0 mol% ZnO glass.

With diiodomethane as a non-polar test liquid, there were no significant differences in the mean contact angles between all ZnO containing glasses and Thermanox®, and 0 mol% ZnO glass as controls.

The term surface energy for solids reflects rather the affinity of the surface to other materials; the higher surface energy of the solid the more energy is gained upon bringing this surface into contact with other materials. Therefore, the surface energy describes the adhesive properties of the material which can be "activated" by different surface treatments (plasma treatment, chemical etching, and hydrogenation) or by changing the material chemistry [29, 32].

The measurement of surface energy is associated with a task of splitting up one material or two different materials being in contact into two parts. This attempt will cause deformation in the bulk material with some energy being dissipated to overcome interatomic forces holding the parts together. The spent energy is connected with the excess energy of the two newly formed interfaces, and theoretically the same amount of energy should be regained when trying to put two parts together. With solids, there is no recovery of this dissipated energy making the measurement of the true value of surface energy impossible. On the other hand for isotropic liquids, where the stress relaxes very quickly, it is possible to measure the true surface energy, and hence the surface energy coincides with the surface tension of the liquid.

In the case of solids, however, it is feasible to measure surface free energy (SFE) rather than the actual surface energy. SFE can be calculated on the basis of contact angle measurements which quantify wettability of the solid materials. This approach involves testing the solid against a series of well characterized wetting liquids in term of the polar and dispersive components of their surface tensions. The relevant equation for surface free energy is given by Owens and Wendt as [29–32]:

$$\gamma_l\ (1 + \cos\ \theta)/(\gamma_{ld})^{1/2} = (\gamma_{sp})^{1/2}\ [(\gamma_{lp})^{1/2}/(\gamma_{ld})^{1/2}] + (\gamma_{sd})^{1/2}$$

where, θ is the contact angle, γ_l is liquid surface tension and γ_s is the solid surface tension, or free energy. The addition of d and p in the subscripts refer to the dispersive and polar components of each, and the total free surface energy is merely the sum of its two component forces. The form of the equation is of the type $y = mx + b$. When $(\gamma_{lp})^{1/2}/(\gamma_{ld})^{1/2}$ plotted versus $\gamma_l\ (1 + \cos\ \theta)/(\gamma_{ld})^{1/2}$; the slope will be $(\gamma_{sp})^{1/2}$ and the y-intercept will be $(\gamma_{sd})^{1/2}$.

The calculated total surface free energy (SFE^{tot}) and its dispersive (SFE^{d}) and polar (SFE^{p}) components are also listed in Table 2. As can be seen, all tested glasses showed significantly higher $SFE^{tot,}$ i.e., highly reactive surfaces compared to Thermanox®. This could be associated with lower contact angles, particularly in H_2O, and the significantly higher polar component of the SFE that these glasses have compared to Thermanox®. Regarding the dispersive component of SFE, there were no significant differences between these glasses (except for 10 mol% ZnO) and Thermanox®. Compared to 0 mol% ZnO glasses, all ZnO containing glasses showed no significant differences in their dispersive, polar, and the total surface free energies.

3.2.2 *Cell viability*

In this study, In vitro viability of MG63 was used to determine the influence of ZnO as a dopant on the cell-glass interactions. Figure 9 shows confocal images of live/

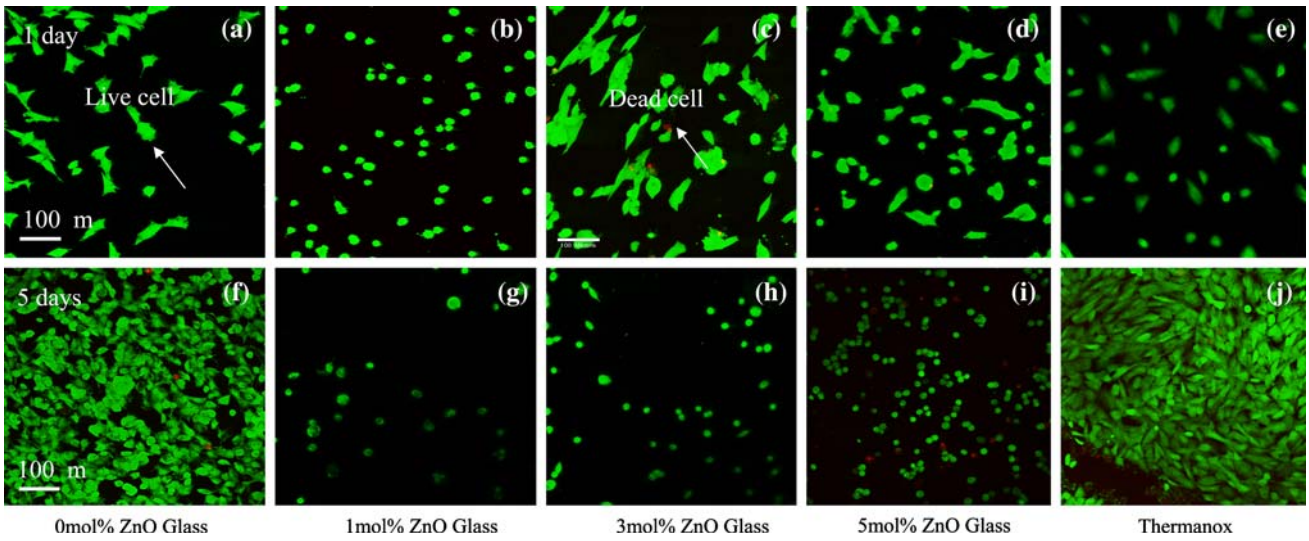

Fig. 9 Confocal images showing viability of MG63 seeded for 1 (**a–e**) and 5 (**f–j**) days on the surface of glass discs with different zinc oxide contents compared to ternary glass discs free from ZnO and Thermanox® positive control

dead stained MG63 cells attached to the surfaces of 0, 1, 3, and 5 mol% ZnO glass compositions, as an example, and the positive control after 1 (Fig. 9a–e) and 5 days (Fig. 9f–j) of culture.

After 1 day of culture and on the surface of 0 mol% ZnO containing glasses, MG63 have well spread morphology and comparable viability to the positive control. On the surface of 1 mol% ZnO containing glasses, MG63 still maintained comparable viability to the positive control, but they have a typical round morphology, indicating that they are not happy to attach to the surface. On 3 mol% ZnO containing glasses, MG63 showed comparable viability and well spread morphology to the positive control. On 5 mol% ZnO glasses, however, MG63 cells showed a comparable viability to the positive control, but the cell morphology is a combination of a typical well spread and round morphology.

After 5 days of culture and on the surface of 0 mol% ZnO containing glass discs, MG63 showed significantly higher viability than those at day 1 of culture. Moreover, the cells still maintained the well spread morphology and formed a flat monolayer. Generally, this composition was still comparable to the positive control regarding both cell viability and morphology. On the surface of 1 and 3 mol% ZnO containing discs, however, the MG63 viability was significantly reduced compared to day 1 of culture, and this was observed by the presence of fewer attached live cells. Regardless of this low viability, no dead cells were detected on these two surfaces, and this could be due to detachment of these cells into the medium due to the relatively high degradation nature of these two compositions. Moreover, MG63 showed the typical round morphology instead of the well spread morphology seen at day 1 of culture for 3 mol% ZnO containing glasses. On 5 mol% ZnO glass surfaces, dead as well as the live cells were detected, and the viability is significantly higher compared to day 1 of culture. Like 1, and 3 mol% ZnO containing glasses, the typical round cell morphology indicated that the cells are not happy to attach to the surface.

Generally, glasses with 10 up to 20 mol% ZnO containing glasses showed lower cell viability at day 1 and 5 of cultures, indicated by increasing the number of dead cells, compared to the Thermanox® (data not shown).

These findings suggested that the 0 mol% ZnO composition offered a biocompatible substrate for MG63 cells to grow. Incorporation of ZnO up to 5 mol% maintained comparable viability at short time point of culture (1 day), but upon long term (5 days), the viability was significantly reduced compared to the positive control. Even though, glasses with ZnO of 5 up to 20 mol% have exactly the same hydrophilicity as 0 mol% ZnO glass indicated by the contact angle, they showed very low cell viability.

The low biocompatibility associated with zinc containing glasses, above 5 mol% ZnO in particular, can be associated with the significant reduction in the pH of the surrounding medium into acidic level after 1 day as observed in another study [15] or release of significant amount of Zn^{2+} which was found to be cytotoxic to MG63 above the level tolerated by these cells. The cytotoxicity of Zn^{2+} was also observed by Ito et al., who concluded that the optimum Zn^{2+} content in Zn/TCP composite must be less than 1.2 wt% when this composite are applied for in vivo application [33]. They also found that 15 mg/L (15 ppm) is more than two times the 50% inhibitive concentration of Zn^{2+} for MC3T3-E1 cells. In another study, Zn^{2+} release in the range of 8 ppm was found to be very

toxic to MG63 cells, and the cytotoxicity of Zn^{2+} caused by the release of lactate dehydrogenase from MG63 cells, index of cytotoxicity, and cell damage via an oxidative stress [34]. This has been also supported by the findings of Sogo et al., who concluded that from the view point of material safety, zinc content should be kept to a minimum level essential to promote bone formation otherwise, the risk of an accidental burst of Zn^{2+} from the material will cause cytotoxicity [35]. As observed from Salih et al., study, the level of Zn^{2+} release increased with both time and the amount of ZnO incorporated into the glass structure [15]. The level of Zn^{2+} release was approximately 50 ppm for 5 mol% ZnO containing glasses after 5 days which is higher than the cytotoxic level observed by both Aina et al. and Ito et al. However, the level of Zn^{2+} release from glasses with less than 5 mol% was close to the cytotoxic level. This may explain the reasonable results seen at day 1 of culture, but the poorer results at day 5 of culture as the Zn^{2+} continues to release.

4 Conclusion

Substitution of Ca^{2+} with Zn^{2+} from 0 to 20 mol% produced a significant increase in density of the glass structure while it reduced the T_g, and melting temperatures. The crystallisation temperature, however, showed a different trend depending on the mol% of substitution, for example, it was significantly increased by 0 to 4 mol% substitution, while it did not show significant changes by 5–20 mol% substitution compared to glasses with no ZnO. Also, glasses with 0 to 4 mol% ZnO showed significantly lower contact angle, however, those with 5–20 mol% ZnO showed no significant differences in the contact angle from 0 mol% ZnO glasses. The ^{31}P and ^{23}Na MAS NMR results suggest that the relative abundances of the Q^1 and Q^2 phosphorus sites are unaffected as CaO is replaced by ZnO in this system, and the local sodium environment also seems to be unaffected by this process on average. The replacement of CaO with ZnO did seem to have the effect of increasing the local disorder of the Q^2 metaphosphate chains, but less so for the Q^1 chain-terminating sites which were already relatively disordered due to the proximity of modifying cations. From the viewpoint of the biological studies, these ZnO containing glasses, in particular 10–20 mol%, showed lower compatibility with MG63 cells compared to both ZnO free and Thermanox®. This low cytocompatibility could be associated with the reduction in the surrounding pH to acidic level [15] and/or release of Zn^{2+} at a level which is toxic to these cells. Therefore, adjusting the glass composition will be considered in our future work to reduce the level of Zn^{2+} release essential to promote bone formation.

Acknowledgment The authors would like to acknowledge the EPSRC for providing the funding to conduct this study.

References

1. L. L. HENCH and J. M. POLAK, *Science* **295**(5557) (2002) 1014
2. J. C. KNOWLES, *J. Mater. Chem.* **13** (2003) 2395
3. K. FRANKS, I. ABRAHAMS and J. C. KNOWLES, *J. Mater. Sci. Mater. Med.* **11** (2000) 609
4. V. SALIH, K. FRANKS, M. JAMES, G. W. HASTINGS, and J. C. KNOWLES, *J. Mater. Sci. Mater. Med.* **11** (2000) 615
5. X. YU, D. E. DAY, G. J. LONG and R. K. BROW, *J. Non-Cryst. Solids* **215** (1997) 21
6. C. S. RAY, X. FANG, M. KARABULUT, G. K. MARASINGHE and D. E. DAY, *J. Non-Cryst. Solids* **249**(1) (1999) 1
7. I. AHMED, C. A. COLLINS, M. P. LEWIS, I. OLSEN and J. C. KNOWLES, *Biomaterials* **25** (2004) 3223
8. E. A. ABOU NEEL, I. AHMED, J. J. BLAKER, A. BISMARCK, A. R. BOCCACCINI, M. P. LEWIS, S. N. NAZHAT and J. C. KNOWLES, *Acta Biomaterialia* **1** (2005) 553
9. E. A. ABOU NEEL, I. AHMED, J. PRATTEN, S. N. NAZHAT and J. C. KNOWLES, *Biomaterials* **26** (2005) 2247
10. R. SHAH, A. C. M. SINANAN, J. C. KNOWLES, N. P. HUNT and M. P. LEWIS, *Biomaterials* **26** (2005) 1497
11. M. NAVARRO, M.-P. GINEBRA and J. A. PLANELL, *J. Biomed. Mater. Res.* **67A** (2003) 1009
12. V. RAJENDRAN, A. V. GAYATHRI DEVI, M. AZOOZ and F. H. EL-BATAL, *J. Non-Cryst. Solids* **353**(1) (2006) 77
13. E. A. ABOU NEEL, T. MIZOGUCHI, M. ITO, M. BITAR, V. SALIH and J. C. KNOWLES, *Biomaterials* **28** (2007) 2967
14. E. A. ABOU NEEL and J. C. KNOWLES, *J Mater. Sci. Mater. Med.* doi: 10.1007/s10856-007-3079-5
15. V. SALIH, A. PATEL and J. C. KNOWLES, *Biomed. Mater.* **2** (2007) 1
16. K. FRANKS, 'The structure and properties of soluble phosphate based glasses, *PhD thesis*, University of London (2000)
17. M. KAMITAKAHARA, C. OHTUSUKI, H. INADA, M. TANIHARA, and T. MIYAZAKI, *Acta Biomaterialia* **2** (2006) 467
18. R. M. DAY and A. R. BOCCACCINI, *J. Biomed. Mater. Res.* **73A** (2005) 73
19. P. PETRINI, C. R. ARCIOLA, I. PEZAALI, S. BOZZINI, L. MONTANARO, M. C. TANZI, P. SPEZIALI and L. VISAI, *Int. J. Artif. Organs* **29**(4) (2006) 434
20. D. MASSIOT, F. FAYON, M. CAPRON, I. KING, S. LE CALVÉ, B. ALONSO, J.-O. DURAND, B. BUJOLI, Z. GAN and G. HOATSON, *Magn. Reson. Chem.* **40** (2002) 70
21. T. F. KEMP, High Field Solid State ^{27}Al NMR of ceramics and glasses. Masters Thesis, University of Warwick (2004)
22. D. R. LIDE, "Handbook of Chemistry and Physics", 74th edn. (The Chemical Rubber Publishing Company, 1993–1994), pp. 4–126 & 12–160
23. P. Y. SHIH, S. W. YUNG and T. S. CHIN, *J. Non-Cryst. Solids* **224** (1998) 143
24. L. A. O'DELL, S. L. P. SAVIN, A. V. CHADWICK and M. E. SMITH, *Appl. Magn. Reson.* **32** (2007) 527
25. R. K. BROW, R. J. KIRKPATRICK and G. L. TURNER, *J. Non-Cryst. Solids* **116** (1990) 39
26. R. K. BROW, C. C. PHIFER, G. L. TURNER and R. J. KIRKPATRICK, *J. Am. Ceram. Soc.* **74** (1991) 1287
27. J. J. BLAKER, V. MAQUET, A. R. BOCCACCINI, R. JÉRÔME and A. BISMARCK, e-polymers (2005) Art No. 23 Apr 1
28. S. WU, "Polymer Interface and Adhesion" (Marcel Dekker, 1982)
29. R. J. GOOD and C. J. Van OSS, in "The Modern Theory of Contact Angles and the Hydrogen Bond Components of Surface

Energies: In Modern Approaches to Wettability edited by M. E. Schrader and G. I. Loeb (Plenum, New York, 1992)
30. F. M. FOWKES, *Ind. Eng. Chem.* **56**(12) (1964) 40
31. F. M. FOWKES, *J. Phys. Chem.* **66**(2) (1962) 382
32. D. K. OWENS and R. C. WENDT, *J. Appl. Polym. Sci.* **13** (1969) 1741
33. A. ITO, K. OJIMA, H. NAITO, N. ICHINOSE and T. TATEISHI, *J. Biomed. Mater. Res.* **50** (2000) 178
34. W. AINA, A. PERARDI, L. BERGANDI, G. MALAVASI, L. MENABUE, C. MORTERRA and D. GHIGO, *Chem. Biol. Interact.* **167** (2007) 207
35. Y. SOGO, T. SAKURAI, K. ONUMA and A. ITO, *J. Biomed. Mater. Res.* **62** (2002) 457